

# Evaluation of submillimeter electromagnetic waves scattering on dust particles in plasma

D. TOADER<sup>a,b</sup>, M. L. MUNTEANU<sup>a</sup>, N. BANU<sup>a,b</sup>, A. SCURTU<sup>a</sup>, C. M. TICOȘ<sup>a,c</sup>

<sup>a</sup> National Institute for Laser, Plasma and Radiation Physics, Bucharest 077125, Romania

<sup>b</sup> University of Bucharest, Department of Physics, 077125, Romania

<sup>c</sup> National Institute for Research and Development for Microtechnologies, Bucharest 077190, Romania

---

The interaction of submillimeter electromagnetic waves with dust particles is studied numerically by evaluating the scattering and absorption coefficients on single spherical grains and on crystalline layers made of spherical microparticles.

(Received December 17, 2012; accepted April 11, 2013)

*Keywords:* Dust particles, Plasma crystal, THz waves

---

## 1. Introduction

Dust particles can be easily levitated between two parallel plate electrodes in a rf plasma. They can form clusters or self arrange in a symmetrical structure called plasma crystal [1-4]. The dimension of the microparticles is of a few microns while the interparticle distance can be from 100 to 500  $\mu\text{m}$ , depending on gas pressure and plasma parameters such as temperature and density of electrons and plasma potential. It was shown that the plasma crystal may be formed in different symmetries such as bcc, fcc, or hcp, set by the neutral gas pressure and rf power [5-6]. A raised interest has been shown in the last years to see how different types of electromagnetic waves interact with plasma crystals. A number of works studied the interaction of UV radiation [7], laser beams [8] and THz waves with crystals [9]. It has been previously predicted that a plasma crystal made of paramagnetic microparticles could be used as a tuning filter for THz waves [10]. By varying the magnetic field, the magnetic force acting on the particles is inducing changes in the structure of the crystal. However in this case the microparticles have high magnetic permeability and are made of materials with low index of refraction which could be a disadvantage. On the other hand the rotation of the crystal due to the ion drag force determined by the ion  $\text{ExB}$  flow could become an inconvenient when a stable structure is sought.

This paper presents some simple preliminary results related to the scattering of THz radiation on dust particles levitated in plasma. Here we do not account for the charge of the particles nor do we consider paramagnetic particles in a magnetic field.

In principle there is a possibility to use such a plasma crystal for tuning THz radiation without an external magnetic field by changing some of the parameters of the

discharge and inducing changes in the interparticle distance.

### 1.1. THz waves

Terahertz (0.5-10 THz) waves have wavelengths in between the infrared spectra and microwaves and are used in different applications such as communications, imaging and spectroscopy [11]. They can be generated in a laboratory setting using a photoconductor junction (PC) illuminated with a femtosecond laser pulse. The valence electrons pass in the conduction band through the absorption of photons and emit radiation in the oscillating field of the laser [12]. The power of the waves emitted by the PC junction is in the nW range which makes it challenging to detect them.

Of importance is to know the scattering efficiency of these electromagnetic waves on a collection of microparticles. The reflection and transmission factors are evaluated numerically when the waves are scattered off a single particle or diffracted by a plasma crystal, as functions of different dust parameters such as the size of the microparticles and the material of which they are made of. This is a very important issue for the experimental scattering and proper detection of the THz waves with a PC junction in a dusty plasma experiment. The condition for using TDS (time-detection-spectroscopy) is to be able to record signals in the scattered waves with sufficiently large amplitude, comparable with that of incident waves.

Moreover, an experiment using THz waves incident on dust particles in plasma should consider the use of specific materials with low absorption coefficient such as Teflon. THz waves are reflected by metals and absorbed by glass, and it is therefore challenging to propagate these waves in a vacuum chamber. The entrance window for THz waves must be made of thick plastic material which needs to be compatible with vacuum.

## 2. Scattering on a sphere

The study of electromagnetic waves starts from the simple case of a single dielectric sphere. By solving the Maxwell equations with the boundary conditions for the electromagnetic field incident and scattered on a sphere in the Mie approximation, one can calculate the scattering, absorption and extinction factors  $Q_{abs}$  and  $Q_{sca}$ , respectively, which are functions of the electromagnetic field amplitude. The scattering coefficient  $Q_{sca}$  can be expressed as [13]:

$$Q_{sca} = \frac{2}{x^2} \sum_{n=1}^{\infty} (2n+1) \left( |a_n|^2 + |b_n|^2 \right) \quad (1)$$

Here,  $a_n$  and  $b_n$  are combinations of the Bessel functions resulted from the series expansion of the electromagnetic field with spherical functions,  $x=2\pi a/\lambda$ , where  $\lambda$  is the wavelength of the electromagnetic waves, and  $a$  is the dust particle radius.  $Q_{sca}$  is defined as:

$$Q_{sca} = \frac{\sigma_{sca}}{\pi a^2}, \quad \frac{d\sigma_{sca}}{d\Omega} = \frac{r^2 P_{sca}}{P_{inc}} \quad (2)$$

where  $\sigma_{sca}$  is the scattering crosssection,  $\Omega$  is the solid angle,  $P_{sca}$  and  $P_{inc}$  are the scattered and incident power, respectively, which are given by:

$$P_{sca} \propto \frac{1}{2} |E_{sca}|^2, \quad P_{inc} \propto \frac{1}{2} |E_{inc}|^2 \quad (3)$$

$E_{sca}$  and  $E_{inc}$  are the scattered and incident electric fields. In the same way, one can infer  $Q_{abs}$ . The evaluation of  $Q_{sca}$  and  $Q_{abs}$  can be done numerically using dedicated codes [14].

The dielectric constant of a dust sphere is defined as:

$$\hat{\epsilon}_r = n^2 \quad (4)$$

and the complex refractive index is

$$\hat{n} = n + ik \quad (5)$$

Therefore the dielectric constant becomes:

$$\epsilon_r = \epsilon'_r + i\epsilon''_r = (n + ik)^2, \quad (6)$$

$$\epsilon'_r = n^2 - k^2 \cong n^2, \quad \epsilon''_r = 2nk \quad (7)$$

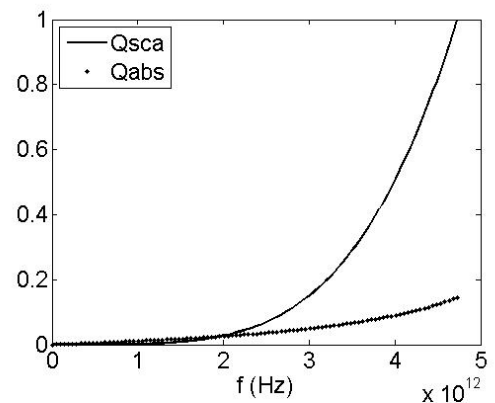
As an example, according to expressions (5-7) for a melamine formaldehyde (MF) sphere we obtain:

$$\epsilon'_r \approx 4.7, n \approx 2.17 \quad (8)$$

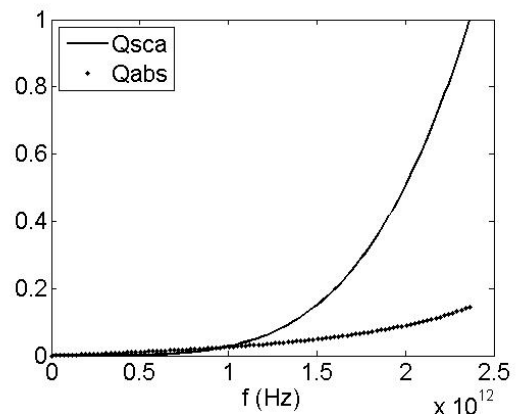
$$\epsilon''_r = \epsilon'_r \operatorname{tg} \delta \quad (9)$$

$$\operatorname{tg} \delta \approx 0.04 \Rightarrow k \approx 0.043 \quad (10)$$

In Figs. 2 a) and (b) the dependencies of the  $Q_{sca}$  and  $Q_{abs}$  coefficients on the frequency in the THz range is shown for MF spheres with two different radii, 10 and 20  $\mu\text{m}$ . One can see that the waves are very strongly scattered above 3 THz for a MF sphere of 10  $\mu\text{m}$  radius while for a larger sphere of 20  $\mu\text{m}$  scattering is more efficient starting at 1.5 THz. As the radius of the sphere is bigger, the maximum value of the scattering coefficient is shifted towards lower frequency values. The absorption coefficient,  $Q_{abs}$ , has a greater value for the larger sphere for the same frequency of the incident waves. For example, the 2 THz wave is absorbed by the 10  $\mu\text{m}$  sphere with a coefficient of 0.01 while for the 20  $\mu\text{m}$  sphere  $Q_{abs}$  is 0.08. The value of 0.15 for the absorption coefficient is found at 4.7 THz for the 10  $\mu\text{m}$  sphere and at 2.35 THz in the case of the larger sphere. Therefore the results show that a smaller microparticle is able to scatter and absorb electromagnetic waves up to 4.5 THz.



(a)



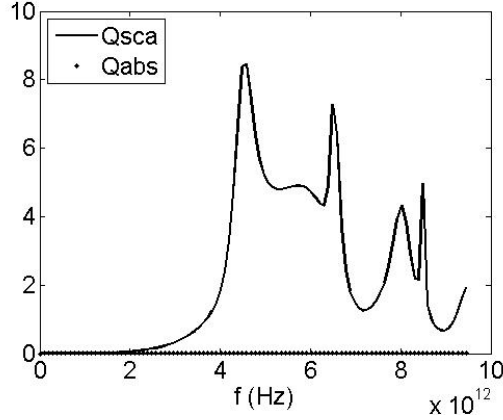
(b)

Fig. 2. (a). Scattering on a MF sphere with radius  $a=10 \mu\text{m}$ ; (b) - Scattering on a MF sphere with  $a=20 \mu\text{m}$ .

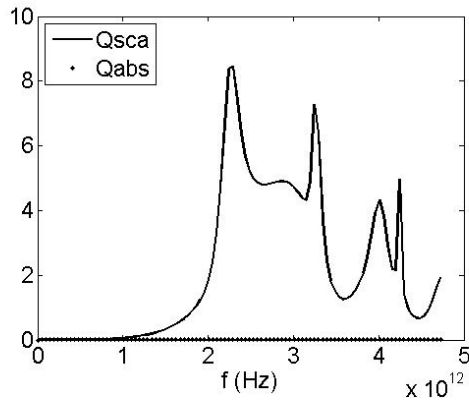
Using the same expressions for alumina ( $\text{Al}_2\text{O}_3$ ) spheres we obtain:

$$\varepsilon'_r \approx 10, n \approx 3.16, \varepsilon''_r = \varepsilon'_r \text{tg} \delta \quad (11)$$

$$\text{tg} \delta \approx 3 \times 10^{-4}, k = \frac{\varepsilon''_r}{2n} \approx 4.7 \times 10^{-4} \quad (12)$$



(a)



(b)

Fig. 3. (a). Scattering on an  $\text{Al}_2\text{O}_3$  sphere with  $a=10 \mu\text{m}$ ; (b). Scattering on an  $\text{Al}_2\text{O}_3$  sphere with  $a=20 \mu\text{m}$ .

Figs. 3 (a) and (b) illustrate the dependence of  $Q_{sca}$  and  $Q_{abs}$  on the waves frequency in the THz range, for  $\text{Al}_2\text{O}_3$  spheres with radii equal to 10 and 20  $\mu\text{m}$ . As can be seen, unlike the MF, the  $\text{Al}_2\text{O}_3$  spheres have a much weaker absorption. The scattering coefficient,  $Q_{sca}$  presents some pair peak values for certain frequencies. For the 10  $\mu\text{m}$  sphere the main peaks appear at approximately 4.5 and 6.5 THz, as shown in Fig. 3 (a). The secondary ones are at 8 and 8.5 THz. Between every set of peaks there is a minimum value. One can see that there is a clear trend in the variation of the scattering coefficient with the frequency of the incident waves. Fig. 3 (b) shows the same behavior for the larger  $\text{Al}_2\text{O}_3$  sphere with a radius of 20  $\mu\text{m}$ . The difference between these two cases is that the peaks of the  $Q_{sca}$  coefficient are shifted towards lower frequencies, i.e. 2.30, 3.25, 4, and 4.25 THz for the larger

microparticle. The bandwidth between these peaks also appears to be narrower.

It can be noted however that because the variable  $x$  depends on the ratio between the dust radius  $a$  and the wavelength  $\lambda$  of the THz waves,  $x$  is invariant when both the dust radius and the wavelength are increased by a factor of 2, as is the case in our simulations. For this reason,  $Q_{sca}$  and  $Q_{abs}$  have the same profiles in the two cases, of  $a$  with  $\lambda$  and  $2a$  with  $2\lambda$  as can be seen in Figs. 2 and 3. The only difference is in the frequency range which is shifted by a factor of 2 as well.

### 3. Scattering on a dust crystal

The scattering of the THz waves on a crystal made up of dust particles is much more complex and cannot be regarded as the sum of individual scatterings. Since the wavelength of the waves is about the same order of magnitude with the inter-grain spacing we can expect Bragg scattering of the waves on a plasma crystal. In this respect we assume that the particles have a still position in the crystal and there are no thermal oscillations similar to the ones present in the atomic crystal lattice. Moreover, multiple scattering is neglected and only diffraction on the crystal layers is considered. Based on these assumptions we further use Bragg scattering theory in the same way diffraction of light on a colloidal crystal made of nanometer size particles is studied [15-16].

An example of crystal produced in plasma is shown in Fig. 4. Here only a horizontal plane of the plasma crystal can be seen. It can be easily observed that the crystal has hexagonal (hcp) symmetry. However it has been demonstrated experimentally that different symmetries can coexist at the same time, such as bcc and fcc [5-6].

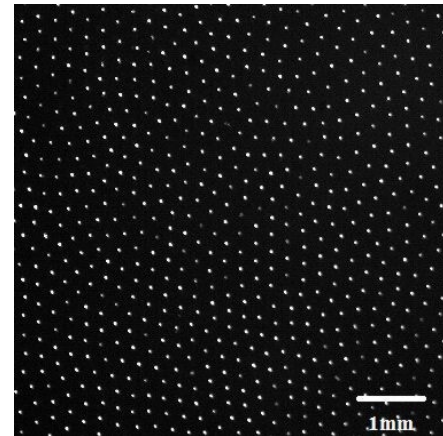


Fig. 4. A horizontal plane in a plasma crystal with hcp symmetry.

The Bragg diffraction law and the reflection and transmission coefficients,  $R$  and  $T$ , of the crystal depend on the crystal properties given by a constant  $A$ :

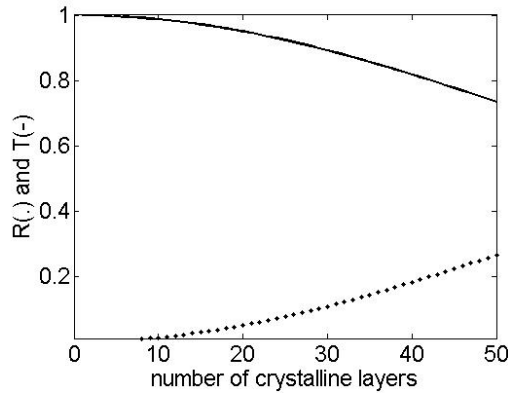
$$N \lambda_0 = 2 \eta D \sin \theta \quad (13)$$

$$R_{\lambda_0} = (\tanh A)^2, T_{\lambda_0} = 1 - R_{\lambda_0} \quad (14)$$

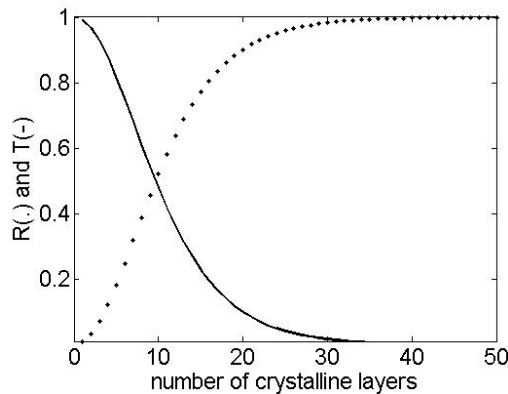
where

$$A = N \frac{2\pi^2 F_H}{\eta \sin^2 \theta} \left( \frac{\varepsilon'_r - 1}{\varepsilon'_r + 2} \right) \left( \frac{a}{\sqrt{3}D} \right) \quad (15)$$

In (15),  $F_H$  depends on the crystal structure. For example in a fcc symmetry  $F_H$  is equal to 4.  $D$  is the distance between the crystal layers,  $\eta$  is the refraction index of the whole crystal ( $\approx 1$ ),  $N$  is the order of the diffraction which is 1 in our case,  $\theta$  is the diffraction angle,  $\varepsilon'_r$  is the dielectric constant of the microparticle material and  $\lambda_0$  is the wavelength.



(a)



(b)

Fig.5. (a) Reflection and transmission coefficients for THz wave scattering on  $\text{Al}_2\text{O}_3$  spheres with radius  $a=10 \mu\text{m}$ ; (b). Reflection and transmission coefficients for THz wave scattering on  $\text{Al}_2\text{O}_3$  spheres with  $a=20 \mu\text{m}$ .

Figs. 5 (a) and (b) give the reflection and the transmission coefficients,  $R$  and  $T$ , respectively, which depend on the number of crystalline layers. The index of refraction for  $\text{Al}_2\text{O}_3$  microspheres is  $n=3.16$ . Two cases are presented: the scattering on a crystal made of spheres with a radius of  $10 \mu\text{m}$  radius and with a radius of  $20 \mu\text{m}$ ,

respectively. In both cases  $D=100 \mu\text{m}$  and  $\lambda_0=100 \mu\text{m}$ . In the first case almost all the incident power of the waves is transmitted for a number up to 15 layers, as shown in Fig. 5 (a). Even for a larger number of layers, of about 50, the transmittance is relatively high ( $\approx 0.75$ ). The absorption becomes important ( $\approx 0.25$ ) at a large number of crystalline planes ( $\geq 50$ ), while being low ( $< 0.1$ ) for up to 10 layers.

In the second case, when large dust particles are used in the crystal, the transmission coefficient is close to 1 for up to 4 layers and then it decreases very rapidly reaching 0.5 for a number of 10 layers, as presented in Fig. 5 (b). For about 30 crystalline layers the crystal becomes opaque to the THz waves and most of the incident wave energy is reflected backward. The reflection coefficient increases rapidly up to 0.5 for a number of approximately 10 layers, and becomes 1 for about 40 layers.

In conclusion, the THz waves are more efficiently reflected by a crystal made of larger microparticles which can act as a reflector for almost all the input energy when a number of more than 25 crystalline layers are present. The THz waves can be efficiently transmitted by a crystal made of spheres with a smaller diameter, even for a large number of layers.

It should be mentioned that  $R$  and  $T$  depend strongly on the factor  $F_H$ . Thus, if locally a structure with bcc symmetry exists, then  $F_H=2$  and the values of  $R$  and  $T$  change significantly. Also it should be noted that the factor  $A$  depends on the ratio  $a/\sqrt{3}D$  and a choice of  $a=10 \mu\text{m}$  and  $D=100 \mu\text{m}$  produces the same results as the set of values  $a=20 \mu\text{m}$  and  $D=200 \mu\text{m}$ .

#### 4. Conclusions

We have shown that the scattering and absorption coefficients of a single microsphere made of MF or  $\text{Al}_2\text{O}_3$  depend on the frequency of the radiation in the range of the THz spectrum. The scattering of THz waves on dust microparticles is more efficient for large enough grains of at least  $10 \mu\text{m}$  in radius. A large dust particle radius is a requirement especially for microparticles made of less absorbing materials like alumina ( $\text{Al}_2\text{O}_3$ ). In the case of plasma crystals the Bragg diffraction is optimum when the radius of the particles relative to the distance between the crystalline layers,  $D$ , is about 0.05. The interparticle distance can be adjusted by a fine tuning of the gas pressure conditions in a dusty plasma, at constant rf power. Further investigations concerning the coexistence of different crystalline structures and their effect during the interaction with THz radiation are needed. Also defects in the lattice structure of the plasma crystal could drastically affect the transmission and reflection coefficients and should be assessed.

#### Acknowledgements

D. Toader, M.L. Munteanu, N. Banu, and A. Scurtu were supported by the National Authority for Scientific Research (ANCS) from contract Nucleu-LAPLAS 2012.

C. M. Ticoş acknowledges support provided by the Sectoral Operational Program Human Resources and Development (SOP HRD) financed from the European Social Fund, and by the Romanian Government under contract POSDRU 89/1.5/S/63700.

## References

- [1] H. Thomas, G. E. Morfill, V. Demmel, J. Goree, B. Feuerbacher, D. Mohlmann, *Phys. Rev. Lett.* **73**, 652 (1994).
- [2] T. Nitter, *Plasma Sources Sci. Technol.* **5**, 93 (1996).
- [3] J. H. Chu, I. Lin, *Physical Review Letters* **72**, 4009 (2004).
- [4] P. K. Shukla, B. Eliasson, *Rev. Mod. Phys.* **81**, 25 (2009).
- [5] J. B. Pieper, J. Goree, R. A. Quinn, *Phys. Rev. E* **54**, 5636 (1996).
- [6] M. Zuzic, A. V. Ivlev, J. Goree, G. E. Morfill, H. M. Thomas, H. Rothermel, U. Konopka, R. Sutterlin, D. D. Goldbeck, *Phys. Rev. Lett.* **85**, 4064 (2000).
- [7] V. N. Tsytovicha, A. P. Nefedov, V. E. Fortov, O. F. Petrov, G. E. Morfill, *Phys. Plasmas* **10**, 2633 (2003).
- [8] A. Melzer, S. Nunomura, D. Samsonov, Z. W. Ma, J. Goree, *Phys. Rev. E* **62**, 4162 (2000).
- [9] S. Ebbinghaus, K. Schröck, J.C. Schauer, E. Bründermann, M. Heyden, G. Schwaab, M. Böke, J. Winter, M. Tani, M. Havenith, *Plasma Sources Sci. Technol.* **15**, 72 (2006).
- [10] M. Rosenberg, D. P. Sheehan, P. K. Shukla, *IEEE Trans. Plasma Sci.* **34**, 490 (2006).
- [11] K. Sakai, *Terahertz Optoelectronics*, Springer-Verlag, Berlin, 2005.
- [12] D. H. Auston, K. P. Cheung, P. R. Smith, *Appl. Phys. Lett.* **45**, 284 (1984).
- [13] H. C. van de Hulst, *Light scattering by small particles*, Dover Publication, Inc., New York, 1981.
- [14] Christian Mätzler, *MATLAB functions for Mie scattering and absorption*, Research Report No. 2002-08, June 2002.
- [15] R. J. Spry, D.J. Kosan, *Appl. Spectroscopy* **40**, 782 (1986).
- [16] P. A. Rundquist, P. Photinos, S. Jagannathan, S. A. Asher, *J. Chem. Phys.* **91**, 4932 (1989).

---

\*Corresponding author: catalin.ticos@inflpr.ro